Progress In Electromagnetics Research C, Vol. 45, 87–100, 2013

DESIGN AND REALIZATION OF THREE-POLE BANDPASS FILTER WITH SPURIOUS RESPONSE SUPPRESSION USING DEFECTED GROUND STRUCTURES

Alia Zakriti[1, *], Naima Amar Touhami[2], Khadija Bargach[2], Mohammed Lamsalli[1], and Mohammad Essaaidi[3]

[1]National School of Applied Sciences, Abdelmalek Essaadi University, Tetuan, Morocco

[2]Faculty of Sciences, Abdelmalek Essaadi University, Tetuan, Morocco

[3]ENSIAS, Rabat, Morocco

Abstract—In this paper, a three-pole bandpass filter (BPF) using a new defected ground structure (DGS) is discussed. The proposed DGS is incorporated in the ground plane under the feed lines and the coupled lines of a bandpass filter to improve the performance of the filter in both passband and stopband. The banpass filter is designed with a center frequency of 1.8 GHz and a bandwidth of 270 MHz. The suppression of better than 20 dB was achieved for frequencies between 2.2 and 5 GHz. A prototype of BPF was fabricated and tested. Prototype measured data was in good agreement with simulation results.

1. INTRODUCTION

Modern microwave communication system requires microstrip bandpass filters with improved performance for out-of-band and in-band responses, high rejection, low insertion loss and reduced size [1, 2]. Defected ground structures (DGS) is one of the new design techniques used to improve the quality of the system [3, 4]. DGS adds an extra degree of freedom in microwave circuit design and opens the door to a wide range of applications. The first DGS was proposed by Park et al. [5], where DGS is designed by connecting two DGS cells with a narrow slot. The effective capacitance and inductance of the transmission line is increased using the DGS which contains wide and narrow etched areas [6, 7].

Received 27 September 2013, Accepted 28 October 2013, Scheduled 31 October 2013

* Corresponding author: Alia Zakriti (alia_zakriti@yahoo.fr).

In the following years, a great lot of novel DGS's were proposed and they had become one of the most interesting areas of research owing to their extensive applicability in microwave circuits [8, 9]. Many passive and active microwave and millimeter devices have been developed to suppress the harmonics and realize the compact physical dimensions of circuits for the design flow of circuits with DGS comparatively simple [10–12].

The defected ground structures may cause the high radiation loss, since the defected ground pattern can operate as a radiator instead of the resonator and the insertion loss increase. Moreover, this radiation problem could be more serious in multilayered PCB. To achieve low radiation losses, the fabricated filter may be enclosed in a metal box. The metal box must be properly dimensioned so that its resonance frequency equals the unwanted resonant frequency of the filter [13].

In this paper, a design of three-pole microstrip bandpass N filter with suppression of spurious band has brought about by considering the wide BPF as a cascading of conventional BPF with DGS Bandstop Filter (BSF). The expected result of a simple BPF together with DGS microstrip is to have a compact bandpass filter with significantly higher spurious responses suppression.

2. THREE-POLE *N* BANDPASS FILTER DESIGN

Figure 1 shows the configuration of the proposed three-pole wide microstrip bandpass N filter. The circuit is etched on a bottom of a RF4 substrate with dielectric constant of 4.3 and a thickness of 1.58 mm. The BPF consists of a three N coupled lines and feeding lines. The overall response of the BPF is determined by coupling

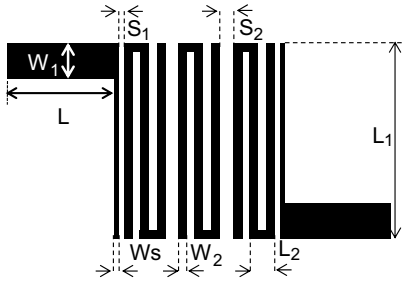

Figure 1. Layout of three-pole N BPF ($W_1 = 3.1$ mm, $W_2 = 0.8$ mm, $W_s = 0.4$ mm, $L_1 = 18$ mm, $L_2 = 2.1$ mm, $S_1 = 0.2$ mm, $S_2 = 0.9$ mm, $L = 10$ mm).

between the resonators. So, the coupling coefficient is related to the spacing between the resonators. The coupling coefficient can be varied by varying spacing between the resonators.

The design of bandpass filter is done for center frequency of 1.8 GHz and a bandwidth of 270 MHz. The simulated results of $3N$ filter are illustrated in Figure 2. The simulation results show a return loss of -10 dB over the passband and an insertion loss of 0.5 dB.

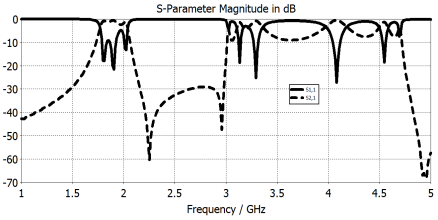

Figure 2. Simulation response of three poles N BPF.

A classic characteristic of distributed filters is higher order responses as we can see clearly at the upper frequency edge of the plot in Figure 2. If the application requires elimination of this band, additional filter elements are required, which can only be accomplished by adding DGS element resonant at desired frequency band rejection.

3. DGS BANDPASS FILTER

Simple microstrip filters have asymmetrical stopbands, and the need for a more complex design can be avoided if DGS elements are used to improve stopband performance. These elements allows the designer to place a zero in the transfer function almost anywhere.

The basic element of DGS is a resonant gap or slot in the ground metal, placed directly under a transmission line and aligned for efficient coupling to the line. Figure 3 shows several resonant structures that may be used. Each one differs in occupied area, equivalent L-C ratio, coupling coefficient, higher-order responses, and other electrical parameters.

This range of structures is used to provide additional rejection at the edges of a filter passband, or at an out-of-band frequency such as a harmonic, mixer image, or any frequency where the filter structure has poor rejection. Similarly, DGS resonators can also be used to remove higher-order responses in directional couplers and power combiner/dividers [14–16].

The view of microstrip with DGS cell is shown in Figure 4(a). The proposed DGS are composed of two $a \times b$ rectangular defected areas,

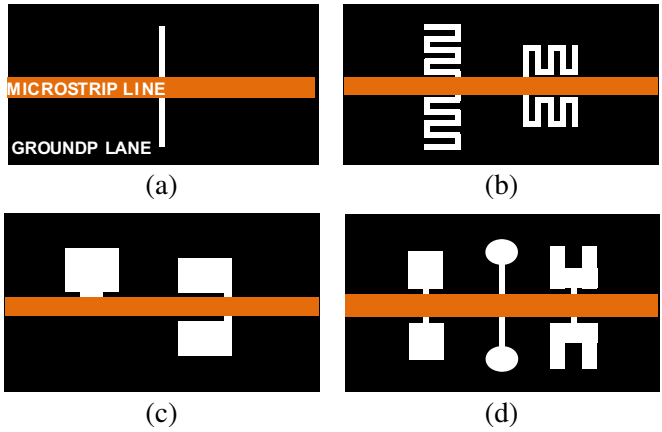

Figure 3. Some common configurations for DGS resonant structures. (a) Slot. (b) Meander lines. (c) Slot variations. (d) Various dumbbell shapes.

$g \times (w+2c)$ gaps. This DGS unit is etched in backside metallic ground plane under the microstrip line. DGS unit can be modeled by a parallel inductive-capacitive (LC) resonant circuit connected to transmission lines at its both sides. In developing this model for the filter, radiation and surface wave losses were also taken into consideration by including parallel resistance R in the equivalent circuit, as shown in Figure 4(b). The values of R, L and C can be computed using the following expressions.

Using the circuit model in Figure 4(b) and the circuit theory, the equivalent impedance of the parallel resonance is given by:

$$Z = Y^{-1} = \left(\frac{1}{R} + j2\pi\left(Cf - \frac{1}{4\pi^2 Lf}\right)\right)^{-1} \tag{1}$$

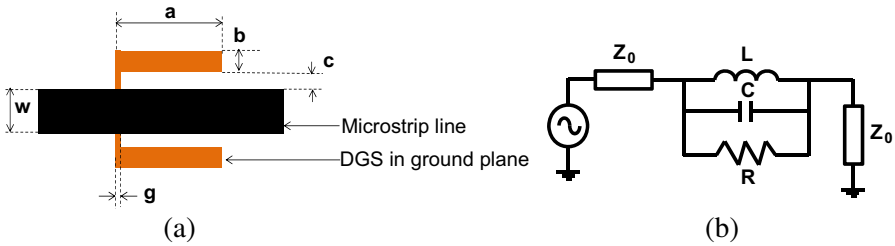

Figure 4. (a) The view of microstrip line with DGS shape. (b) Equivalent circuit of DGS cell.

The transmission coefficients are then calculated as follows:

$$S_{12} = \frac{1}{1 + \frac{1}{2} Z Z_0^{-1}} \tag{2}$$

For

$$R \gg Z_0 \quad \rightarrow \quad Z = \left(j2\pi \left(Cf - \frac{1}{4\pi^2 Lf} \right) \right)^{-1} \tag{3}$$

$$|S_{12}| = \left[1 + (2Z_0)^{-2} \left(4\pi^2 \left(\frac{1}{4\pi^2 fL} - fC \right)^2 \right)^{-1} \right]^{\frac{1}{2}}$$

$$= \left[1 + (2Z_0)^{-2} \left(\frac{1}{\omega L} - \omega C \right)^{-2} \right]^{\frac{-1}{2}} \tag{4}$$

At resonant frequency, the relationship between LC and ω_0 is defined as follows:

$$L = \frac{1}{\omega_0^2 C} \tag{5}$$

Substituting this result in the Eq. (4), gives:

$$|S_{12}| = \left[1 + (2Z_0)^{-2} \left(\frac{L(\omega\omega_0)^2}{\omega \left(\omega_0^2 - \omega^2 \right)} \right)^2 \right]^{\frac{1}{2}} = \left[\frac{1}{\sqrt{2}} \right]_{\omega=\omega_c} \tag{6}$$

Using Eqs. (6) and (5), the capacitance and inductance of the equivalent-circuit model can be given by:

$$L = \frac{2Z_0}{\omega_0^2} \left[\frac{\left(\omega_0^2 - \omega_c^2 \right)}{\omega_0} \right] \quad \text{and} \quad C = \frac{1}{2Z_0} \left[\frac{\omega_c}{\left(\omega_0^2 - \omega_c^2 \right)} \right] \tag{7}$$

The resistance R in the equivalent circuit model is best fitted around the resonant frequency ω_0. In this case, the equivalent circuit impedance is $Z = R$ (Eq. (1)), which yields:

$$R = 2Z_0 \left[\left(S_{12}|_{\omega=\omega_0} \right)^{-1} - 1 \right] \tag{8}$$

The values of f_0, f_c and $S_{12}|_{\omega=\omega_0}$ are easily extracted from the EM-simulation curve of the DGS element.

4. DGS-ENHANCED FILTER

The presence of spurious bands is a fundamental limitation of microwave filters. As we can see in Figure 2, the first spurious band is relatively close to the frequency range of interest and the unwanted spurious bands appears in the higher frequencies. The spurious responses can be rejected by the use of one DGS unit but when two identical DGS are introduced at both ends of the feed lines, this unwanted band is suppressed with better attenuation [17]. Consequently, two identical cell DGS are incorporated in the ground plane under both input and output feed lines of a simple coupled N lines bandpass filter. This integrated circuit is shown in Figure 5 where each DGS unit is placed at a distance d from the edge of the feed lines.

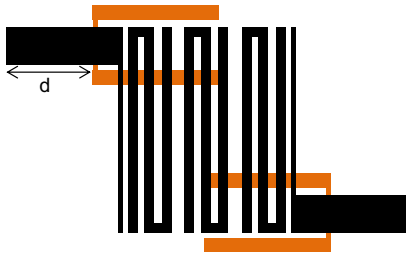

Figure 5. Layout of three poles N BPF on two DGS units.

In order to enhance the spurious response rejection of the proposed filter, we choose to study the effect of DGS dimensions. Then, we vary one dimension of the DGS cell and keeping other dimensions fixed. Plots of the S-parameters with different length of the rectangular defected areas, which is indicated by a parameter (Figure 4), are shown in Figure 6. We can see that the best result is obtained for a parameter equal to 9 mm.

Plots of the S-parameters with different width of the rectangular defected areas, which is indicated by b parameter (Figure 4) are shown in Figure 7. We can see that the best result is obtained for b parameter equal to 2 mm.

Figure 8 represents the S-parameters with different values of the gap coefficient c (Figure 4). We can see that the best result is obtained for c parameter equal to 0.4 mm.

Plots of the S-parameters with different width of the gap, which is indicated by g parameter (Figure 4) are shown in Figure 9. We can see that the best result is obtained for g parameter equal to 0.2 mm.

Plots of the S-parameters with different d parameter (Figure 5)

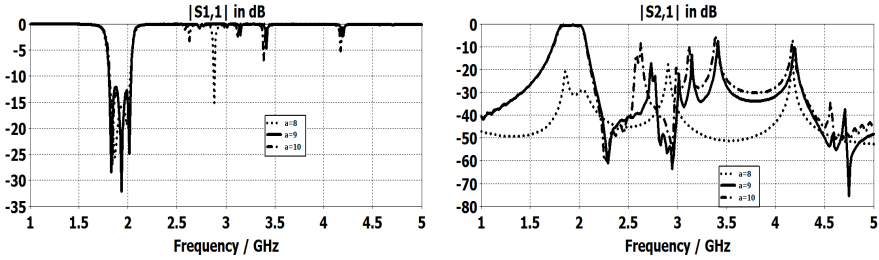

(a) (b)

Figure 6. Investigate parameter a (varies a, $b = 2\,\text{mm}$, $c = 0.4\,\text{mm}$, $g = 0.2\,\text{mm}$ and $d = 5.5\,\text{mm}$) (Dotted $a = 8\,\text{mm}$, solid $a = 9\,\text{mm}$, Dash dotted $a = 10\,\text{mm}$). (a) Return loss. (b) Insertion loss.

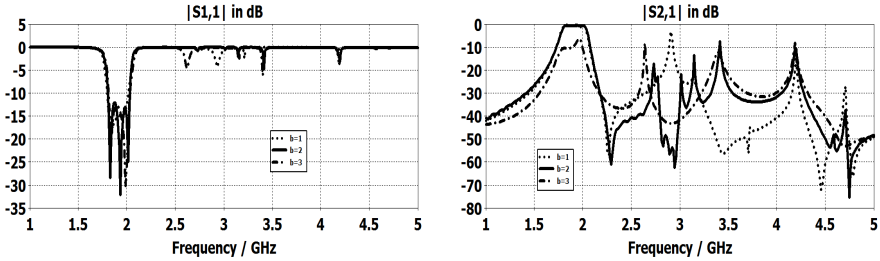

(a) (b)

Figure 7. Investigate parameter b ($a = 9\,\text{mm}$, varies b, $c = 0.4\,\text{mm}$, $g = 0.2\,\text{mm}$ and $d = 5.5\,\text{mm}$) (Dotted $b = 1\,\text{mm}$, solid $b = 2\,\text{mm}$, Dash dotted $b = 3\,\text{mm}$). (a) Return loss. (b) Insertion loss.

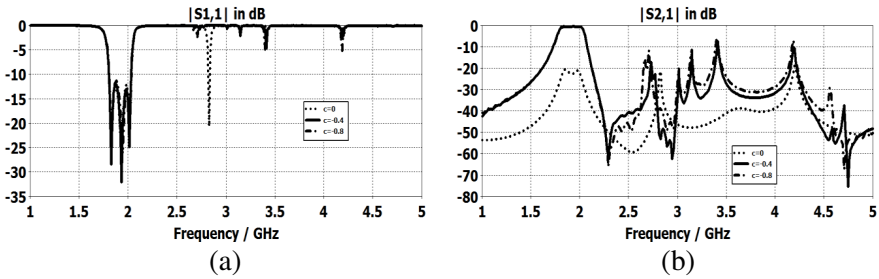

(a) (b)

Figure 8. Investigate parameter c ($a = 9\,\text{mm}$, $b = 2\,\text{mm}$, varies c, $g = 0.2\,\text{mm}$ and $d = 5.5\,\text{mm}$) (Dotted $c = 0\,\text{mm}$, solid $c = 0.4\,\text{mm}$, Dash dotted $c = 0.8\,\text{mm}$). (a) Return loss. (b) Insertion loss.

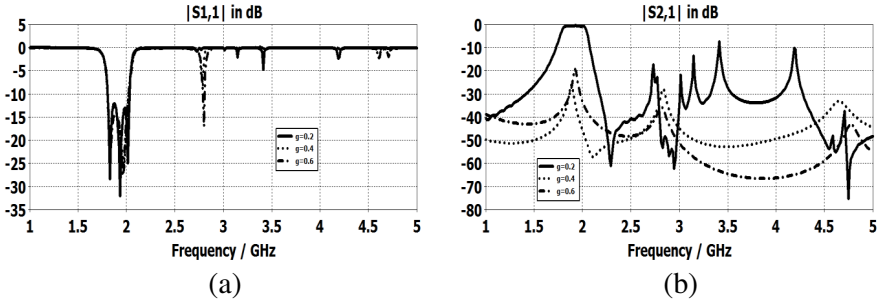

(a) (b)

Figure 9. Investigate parameter g ($a = 9\,\text{mm}$, $b = 2\,\text{mm}$, $c = 0.4\,\text{mm}$, varies g and $d = 5.5\,\text{mm}$) (Solid $g = 0.2\,\text{mm}$, Dotted $g = 0.4\,\text{mm}$, Dash dotted $g = 0.6\,\text{mm}$). (a) Return loss. (b) Insertion loss.

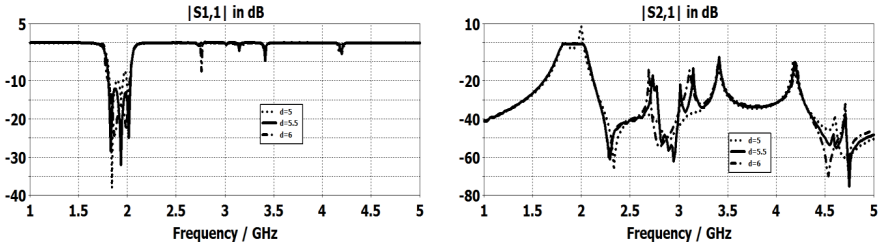

(a) (b)

Figure 10. Investigate parameter d ($a = 9\,\text{mm}$, $b = 2\,\text{mm}$, $c = 0.4\,\text{mm}$, $g = 0.2\,\text{mm}$ and varies d) (Dotted $d = 5\,\text{mm}$, solid $d = 5.5\,\text{mm}$, Dash dotted $d = 6\,\text{mm}$). (a) Return loss. (b) Insertion loss.

Table 1. DGS parameters.

a	B	C	g
9 mm	2 mm	0.4 mm	0.2 mm

are shown in Figure 10. We can see that the best result is obtained for d parameter equal to 5.5 mm.

Consequently, the greatest response used to improve the spurious response suppression occurs for the following DGS parameters.

The DGS dimensions optimized for desired performance are summarized in Table 1.

As seen in Figure 11, the simulated S-parameters of the proposed DGS unit, show the one-pole stopband filter characteristics with an attenuation pole around 4 GHz and 3 dB cutoff frequencies at 3.6 GHz and 4.8 GHz. This one-pole in frequency response will be used to

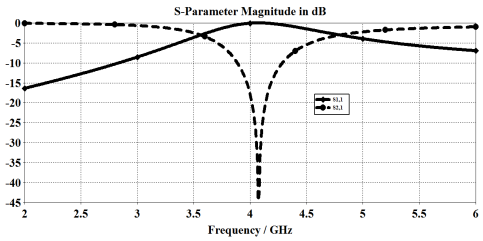

Figure 11. Simulated S-parameters of DGS resonator.

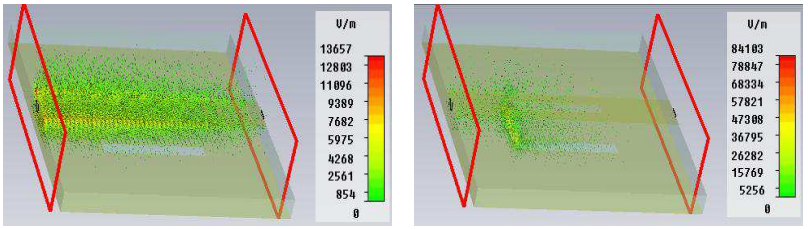

(a) (b)

Figure 12. E-field transmission of the DGS. (a) Snapshot of E-field transmission at 1.8 GHz. (b) Snapshot of E-field transmission at 4.1 GHz.

provide rejection of the spurious responses of a bandpass N filter.

Figure 12 shows the snapshot of simulation at various frequencies of the E-field transmission of the DGS shaped having the dimensions as shown in Table 1. The E-field snapshot at 1.8 GHz shown in Figure 12(a) depicts that at 1.8 GHz, the signal is allowed to pass through as represented by the green color. The E-field snapshot at 4.1 GHz shown in Figure 12(b) depicts that at 4.1 GHz the signal is not allowed to pass through and no output is obtained at the other end.

The simulated S-parameters of three-pole N BPF with two-cells DGS are shown in Figure 13. When compared with the response of the simpler filter (Figure 2), it is easy to see the improvement of passband performances and better spurious responses suppression below -10 dB.

To further enhance the stopband performance of this filter, one other cell DGS is etched in the center of ground plane under the coupled lines of the N filter as seen in Figure 14.

A wide stopband is clearly observed from the simulated plots of Figure 15 with a rejection of 20 dB or higher from 2.2 GHz to 5 GHz. The filtering performance has dramatically improved by the introduction of the third DGS cell.

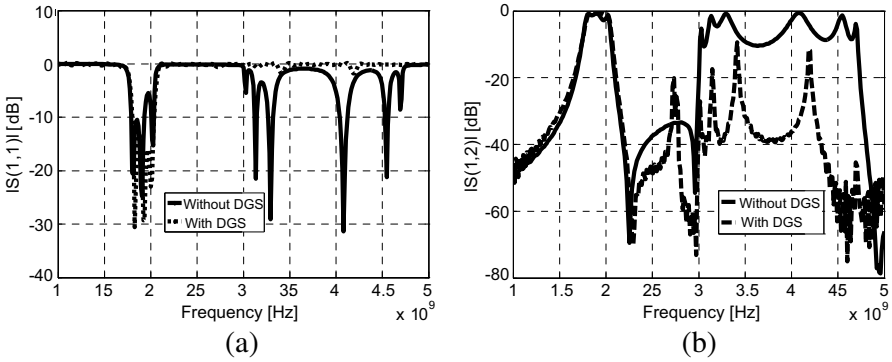

Figure 13. Comparison of simulated S parameters of three poles N lines BPF with and without two DGS units. (a) Return loss. (b) Insertion loss.

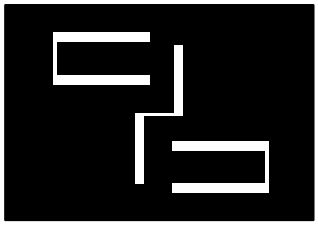

Figure 14. The bottom view of the proposed filter with three-cell DGS.

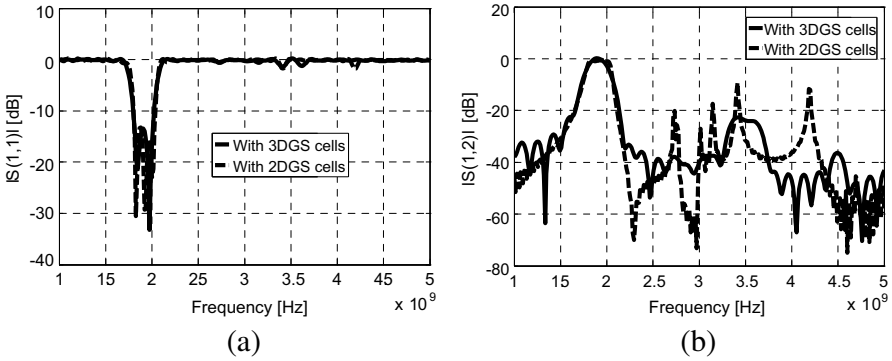

Figure 15. Comparison of simulated S parameters of three poles N lines BPF with two and three DGS units. (a) Return loss. (b) Insertion loss.

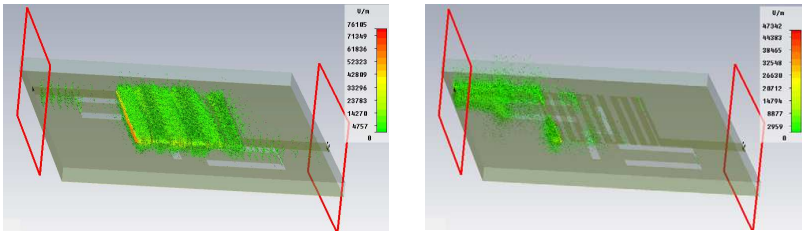

(a) (b)

Figure 16. *E*-field transmission of the threepoles *N* lines BPF with three DGS. (a) Snapshot of *E*-field transmission at 1.8 GHz. (b) Snapshot of *E*-field transmission at 4.1 GHz.

Figure 16 shows the snapshots of simulation of the *E*-field transmission by the three poles *N* lines BPF with three DGS units at various frequencies. The *E*-field snapshot at 1.8 GHz shown in Figure 16(a) depicts that at 1.8 GHz the signal is allowed to pass through by the proposed filter. The *E*-field snapshot at 4.1 GHz shown in Figure 16(b) depicts that at 4.1 GHz the signal is not allowed to pass through by the filter. The objective of the present work to suppress the spurious responses around 4.1 GHz is thus achieved.

The prototype structure of three-pole *N* lines BPF with three-cell DGS is fabricated on FR4 substrate with a relative dielectric constant of 4.3 and a thickness *h* of 1.58 mm. Measurements were carried out using Rohde and Schwarz ZVB 20 vector network analyzer. The prototype views of the Top plane and Ground plane are shown in the Figures 17(a) and 17(b), respectively.

(a) (b)

Figure 17. Fabricated three-pole *N* lines BPF with three-cell DGS. (a) Top view. (b) Bottom view.

Both the simulated and measured *S*-parameters are plotted in Figure 18. The measured results show good agreement with simulation

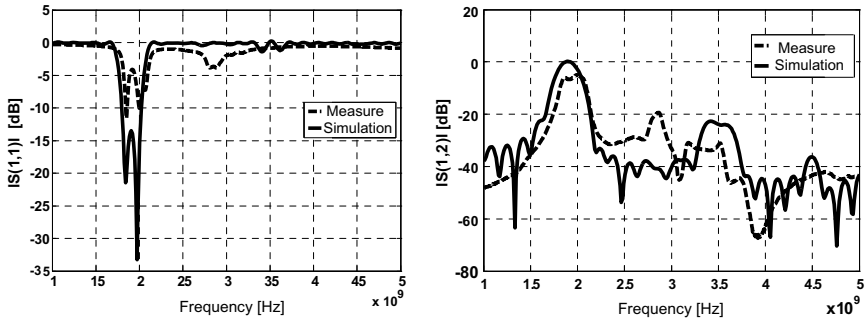

Figure 18. Comparison between simulated and measured S parameters of three poles N lines BPF with three DGS cells. (a) Return loss. (b) Insertion loss.

results. The fabricated BPF has a center frequency of 1.8 GHz and a suppression level of 20 dB from 2.2 GHz to 5 GHz. Consequently, we have demonstrated that the proposed bandpass filter incorporating DGS cells has highly improved performance over the conventional bandpass filter (Figure 2).

5. CONCLUSIONS

A new three-pole N lines bandpass filter with defected ground structure is introduced in this paper. The design center frequency of 1.8 GHz and an operating bandwidth of 270 MHz. The conventional bandpass filter was designed first with associated simulation results that showed the expected unwanted passband.

Cascading DGS with that three poles N lines BPF improved the performance of the filter over the desired passband and increased the suppression of unwanted wide band. The simulation results showed an insertion loss of less than 0.5 dB and return loss of 10 dB of better. The use of DGS cells shows suppression better than 20 dB over the unwanted passband without any degradation over the design operating. The filters were designed, fabricated and tested. Good agreement between simulated and measured results was achieved.

REFERENCES

1. Hunter, I. C., "Microwave filters applications and technology," *IEEE Trans. on Microwave Theory and Tech.*, Vol. 50, No. 3, 794–805, 2002.

2. Garcia-Garcia, J., F. Martin, F. Falcone, J. Bonache, J. Baena, I. Gil, E. Amat, T. Lopetegi, M. Laso, J. Iturmendi, M. Sorolla, and R. Marquies, "Microwave filters with improved stopband based on sub-wavelength resonators," *IEEE Trans. on Microwave Theory and Tech.*, Vol. 53, 1997–2006, 2005.
3. Oraizi, H. and M. S. Esfahlan, "Miniaturization of Wilkinson power dividers by using defected ground structures," *Progress In Electromagnetics Research Letters*, Vol. 4, 113–120, 2008.
4. Wu, B., B. Li, T. Su, and C. H. Liang, "Study on transmission characteristic of split ring resonator defected ground structure," *Progress In Electromagnetics Research*, Vol. 50, 710–714, 2006.
5. Park, J. I., C. S. Kim, J. S. Park, Y. Qian, D. Ahn, and T. Itoh, "Modeling of photonic bandgap and its application for the low-pass filter design," *1999 Asia Pacific Microwave Conference*, 331–334, Dec. 1999.
6. Joung, M. S., J. O. Kim, J. S. Park, J. B. Lim, and H. G. Cho, "A novel defected ground structure and its application to a microwave oscillator," *33th European Microwave Conference*, 781–784, Oct. 2003.
7. Joung, M. S., J. O. Kim, J. S. Park, J. B. Lim, and H. G. C:ho, "A design of the self oscillation mixer using a novel DGS," *Asia Pacific Microwave Conference*, Vol. 2, 8136–889, Nov. 2003.
8. Boutejdar, A., A. Elsherbini, A. Balalem, J. Machac, and A. Omar, "Design of new DGS hairpin microstrip bandpass filter using coupling matrix method," *PIERS Proceedings*, 261–265, Prague, Czech Republic, Aug. 27–30, 2007.
9. Xiao, J.-K. and Y.-F. Zhu, "New U-shaped DGS bandstop filters," *Progress In Electromagnetics Research C*, Vol. 25, 179–191, 2012.
10. Garcia, J., F. Martin, F. Falcone, J. Bonache, I. Gil, T. Lopetegi, M. A. G. Laso, M. Sorolla, and R. Marquies, "Spurious passband suppression in microstrip coupled line band pass filters by means of split ring resonators," *IEEE Microw. Wireless Compon. Lett.*, Vol. 14, No. 9, 416–418, 2004.
11. Lopetegi, T., M. A. G. Laso, J. Hernandez, M. Bacaicoa, D. Benito, M. J. Garde, M. Sorolla, and M. Guglielmi, "New microstrip wiggly-line filters with spurious passband suppression," *IEEE Trans. on Microwave Theory and Tech.*, Vol. 49, 1593–1598, 2001.
12. Kuo, J. T. and W. Hsu, "Parallel coupled microstrip filters with suppression of harmonic response," *IEEE Microw. Wireless Compon. Lett.*, Vol. 12, No. 10, 383–385, 2002.

13. Boutejdar, A. and A. Omar, "Compensating for DGS filter loss," *Microwaves & RF Journal*, Feb. 2012.
14. Woo, D.-J. and T.-K. Lee, "Suppression of harmonics in Wilkinson power divider using dual-band rejection by asymmetric DGS," *IEEE Trans. on Microwave Theory and Tech.*, Vol. 53, No. 6, 2139–2144, Jun. 2005.
15. Kulkarni, M. G. and N. Sarwade, "Suppression of harmonics in Wilkinson power divider using defected ground structures," *International Journal of Electronics and Communication Technology*, Vol. 2, No. 2, Jun. 2011.
16. Sung, Y. J., C. S. Ahn, and Y.-S. Kim, "Size reduction and harmonic suppression of rat-race hybrid coupler using defected ground structure," *IEEE Microw. Wireless Compon. Lett.*, Vol. 14, No. 1, Jan. 2004.
17. Banerji, A., "Design of a wide stop-band harmonic suppressed microstrip low pass planar filter using defected ground structure," *International Journal on Electrical Engineering and Informatics*, Vol. 4, No. 1, Mar. 2012.